ChemComm

Reversible Mechanochromic Luminescence and Aggregation Induced Emission for a Metal-Free β-Diketone

Journal:	*ChemComm*
Manuscript ID:	CC-COM-11-2014-009439.R1
Article Type:	Communication
Date Submitted by the Author:	31-Dec-2014
Complete List of Authors:	Butler, Tristan; University of Virginia, Department of Chemistry Morris, William; University of Virginia, Department of Chemistry Samonina-Kosicka, Jelena; University of Virginia, Department of Chemistry Fraser, Cassandra; University of Virginia, Department of Chemistry

Journal Name

RSCPublishing

COMMUNICATION

Mechanochromic Luminescence and Aggregation Induced Emission for a Metal-Free β-Diketone

Cite this: DOI: 10.1039/xoxxoooooox
Received ooth January 2012,
Accepted ooth January 2012
DOI: 10.1039/xoxxoooooox
www.rsc.org/

Tristan Butler, William A. Morris, Jelena Samonina-Kosicka, Cassandra L. Fraser

Reversible mechanochromic luminescence (ML) is known for difluoroboron β-diketonates (BF_2bdks). Here, we report ML for the methoxy-substituted dinaphthoylmethane (dnmOMe) ligand even without coordination to boron. In addition, dnmOMe shows solvatochromism and aggregation-induced emission (AIE). Diketone thin films showed high contrast emission when smeared, and rapid recovery of the pre-smeared state at room temperature

Organic luminescent materials have been studied extensively for their potential use in optical and optoelectronic devices.[1] Many of these applications require stimuli responsive materials with broad wavelength coverage[2] and efficient solid-state emission.[1, 3] One class of stimuli responsive systems are mechanochromic luminescent (ML) materials that change emission wavelength when subjected to external mechanical forces such as smearing or grinding. Compounds that show ML are of interest for applications such as sensors, security inks, shape memory materials and light-emitting diodes.[4] There are numerous types of ML materials including liquid crystals,[5] polymers,[6] inorganic[7] and organic systems.[8] Often, dynamic ML materials are designed with electron donor and acceptor motifs in order to modulate ML properties.[9] For example, tetrathiazolylthiophene ML materials have been engineered to show distinct optical responses to different types of applied pressure, which demonstrates the potential for practical applications as mechanical sensors.[10]

Materials that exhibit solid-state emission, an inherent quality required for ML materials, have been difficult to realize because many fluorophores that are emissive in solution suffer from aggregation caused quenching (ACQ).[11] Instead of emitting a photon, ACQ dyes dissipate energy through non-radiative pathways and intermolecular interactions in aggregate species.[1, 12]

One strategy to overcome ACQ is to design materials with aggregation induced emission (AIE).[13] The term AIE was coined by Tang *et al* using a hexaphenylsilole (HPS) system. While not emissive in solution, as a solid it showed bright emission.[13-14] This phenomenon was attributed to the restriction of intramolecular motions (RIM) upon dye aggregation.[14-15] Since this initial discovery many different types of AIE active organic materials have been developed including triarylamine,[16] tetraphenylethene,[17] silole,[13, 18] and cyanostilbene[19] based materials. Recently, materials showing AIE have proven useful for applications such as OLEDs,[20] bioprobes,[21] and bioelectronics.[22] Many of these systems show ML in addition to AIE.[23]

Previously, we described difluoroboron coordinated β-diketonates (BF_2bdk) with efficient solid-state emission that also exhibit ML.[24] Furthermore, these materials can self heal at room temperature and be smeared and erased multiple times without degradation.[25] The effects of arene size,[26] alkyl chain length[27] and halide substitution,[28] have been investigated. A current model proposed by Zhang *et al*.[29] attributes BF_2bdk ML behavior to face-to-face H-aggregates that act as low energy emitters. A recent study shows AIE in addition to ML for the difluoroboron complex of 1-phenyl-3-(3,5-dimethoxyphenyl)-propane-1,3-dione which further demonstrates the versatility of BF_2bdk materials.[30]

In the course of exploring substituent and processing effects on ML properties for BF_2bdk complexes it was discovered that dnmOMe shows ML absent coordination to boron. High contrast blue-green emission is visible when dnmOMe thin films are exposed to a mechanical stimulus. This also dye exhibits AIE. Properties of boron-free dnmOMe are presented below.

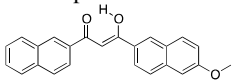

Methoxy-dinaphthoylmethane, dnmOMe, was prepared via Claisen condensation from 6′-methoxy-naphthanone and methyl-2-naphthoate. The ligand dnmOMe was isolated as a light tan-colored powder that is soluble in common organic solvents such as THF, acetone, CH_2Cl_2, and DMSO. The absorption and emission spectra of dnmOMe were recorded in CH_2Cl_2 (S4). In solution, the optical properties of dnmOMe are unremarkable. An absorption peak is observed at 378 nm with a molar absorptivity of 34000 $M^{-1}cm^{-1}$. To the eye, dnmOMe appeared non-emissive, however a peak was observed at 443 nm in the emission spectrum. The quantum yield of dnmOMe in CH_2Cl_2 was negligible (Φ□~0.002). Lifetime measurements of dnmOMe solutions showed short lifetimes (τ = 0.18 ns) and multi-exponential decay, which suggests that multiple emissive species are present in solution. One possible explanation for this observation is that emissions from both keto and enol forms are detected. Both forms are observed in the ^{1}H NMR spectrum, as previous reported for bdks. [31] Different naphthyl ring rotomers are also possible.

Density functional theory (DFT) calculations of the HOMO and LUMO molecular orbitals using B3LYP/6-31G(d) point to an

intramolecular charge transfer (ICT) transition from the methoxy substituted major donor ring to the rest of the molecule, suggesting solvatochromism might be present for dnmOMe (Fig. 1). To explore this possibility, absorption and emission spectra of dnmOMe were

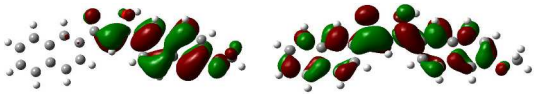

Fig 1. HOMO (left) and LUMO (right) molecular orbitals of dnmOMe.

measured in a variety of solvents with a dnmOMe concentration of 10^{-5} M (Fig 2). The peak absorptions of dnmOMe showed maxima between 378-379 nm and similar relative absorption intensities ranging from 1.69 in toluene to 1.91 in THF. Under UV-excitation dnmOMe showed no emission in nonpolar solvents. As the solvent polarity was increased, blue emission is evident. The emission spectra showed a bathochromic shift from 422 nm in hexanes to 466 nm acetonitrile and the emission intensity was larger in polar solvents. The data were fit according to Lippert-Mataga[32] theory in order to further evaluate the solvatochromic behavior in dnmOMe (S5). The plot of Stokes shift ($\Delta\nu$) versus the solvent polarity parameter (Δf) shows a slightly positive trend with a slope of 1850 indicating moderate solvatochromism. In addition to solvatochromism, dnmOMe shows sensitivity to base due to the acidic proton in uncoordinated β-diketones (e.g. α methylene or enol depending on the tautomer). Emission in CH_3CN is quenched upon the addition of triethylamine (TEA) and can be recovered with the addition of acetic acid (S6).

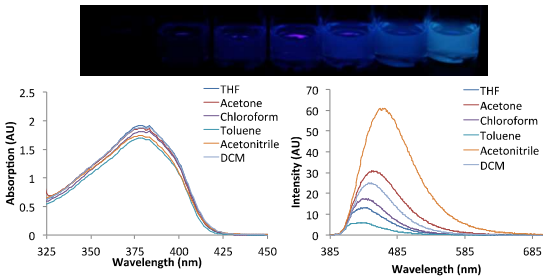

Fig 2. Top: UV excited dnmOMe in different solvents, from left to right: toluene, CH_2Cl_2, acetone, THF, $CHCl_3$, CH_3CN. Bottom: Absorption and emission spectra of dnmOMe (10^{-5} M) in different solvents (λ_{ex} = 369 nm).

The AIE properties of dnmOMe were investigated by measuring the absorption (S7) emission (S8) spectra of THF/H_2O mixtures with increasing H_2O fractions (Fig. 3).[33] As the water fraction was increased from 0-70% a gradual increase in emission intensity was observed which demonstrates AIE behavior for dnmOMe. Over nearly the same water fraction range, a 47 nm red-shift in emission wavelength from 438 nm in pure THF (blue) to 485 nm in 80% water (blue-green) was observed. When the water fraction was increased above 70% the solution became cloudy accompanied by a dramatic decrease in emission intensity and a hypsochromic wavelength shift. At this point, it is likely that aggregates reached a critical size and dnmOMe precipitate is formed. As more aggregates precipitated out of solution the emission decreased until eventually, in 100% water, the mixture was essentially non-emissive.

Though dnmOMe shows AIE, in the solid state pristine samples appeared non-emissive to the eye. This suggests that optical properties of dnmOMe solids are sensitive to molecular packing and different optical properties may be accessible through mechanical perturbation. The ML properties of dnmOMe were explored using spin-cast films on glass prepared from a 10^{-3} M THF solution as previously described.[34] The annealing temperature was determined

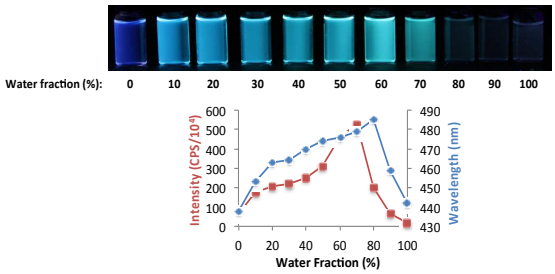

Fig 3. Top: THF/H_2O dnmOMe mixtures with increasing water fractions. Bottom: Plot of emission intensity (red) and peak emission wavelength (blue) versus water fraction.

experimentally by monitoring the peak wavelength as a function of temperature (S9)[28]. Though the dnmOMe emission maximum was largely independent of annealing temperature, the full width at half maximum (FWHM) was minimized at 140°C, thus samples were annealed at this temperature. DSC thermograms show that dnmOMe has a melting point (T_m) of 164 °C and crystallization temperature (T_c) of 126 °C so it is not required to heat dnmOMe thin films above T_m to anneal and change the optical properties and presumably aggregation state of the sample (S10). After cooling to room temperature, annealed samples were gently smeared with a cotton swab to induce a bathochromic shift in emission.

The optical properties and solid-state quantum yields of dnmOMe in as spun (AS), thermally annealed (TA) and smeared (SM) states were also measured. In the as spun state (i.e. prior to annealing), films of dnmOMe showed faint blue emission (Fig. 4) (λ_{em} = 475 nm, FWHM = 109 nm, Φ = 3.3%). After the sample was annealed at 140 °C, no luminescence was observable to the eye, yet emission spectra showed a broad peak at 440 nm (FWHM =136 nm, Φ = 3.6%). Some fine structure emerged in the blue-shifted portion (385- 480 nm) of the spectrum, however a shoulder was observed near 500 nm, which contributed to the increased FWHM observed in the annealed state. In contrast, the smeared state of dnmOMe was blue-green in color with a peak emission of 503 nm and FWHM of 165 nm, which was broader than observed for AS and TA states. Furthermore, the quantum yield increased to 10.6% compared to 3.3% and 3.6% in the AS and TA states, respectively. A contrast ratio of 22.8 was estimated for dnmOMe by comparing the ratio of the peak intensities in the SM and TA states (S11).[35] Pre-exponential weighted lifetimes of dnmOMe were also measured for the films in different states. Decay curves for solid state emission were fit to multi-exponential functions indicating the formation of ground-state dimers or excimers which is typical for solid state luminescence.[29, 36] In the AS state, dnmOMe exhibited a lifetime of 4.7 ns, which decreased to 1.2 ns after annealing. Upon smearing, the lifetime increased to 2.3 ns. Excitation spectra of dnmOMe in each state monitored at 504 nm were also collected (S12). The shape of each excitation spectrum is similar, however the peak intensity for the SM sample was higher than for AS and TA samples.

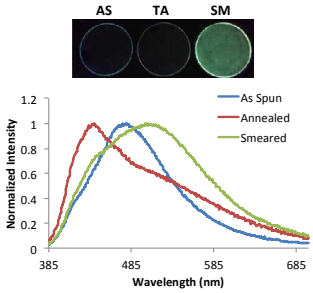

Fig 4. Thin films of dnmOMe (top) and emission spectra corresponding to as spun, thermally annealed, and smeared states (bottom) (λ_{ex} = 369 nm).

Previously, certain smeared BF_2bdks thin films have been shown to spontaneously recover the initial (i.e. annealed) emissive state under ambient conditions.[24-25, 27] This dynamic erasing property is tunable through molecular structure and processing, making it attractive for use in certain applications. Since dnmOMe contains the same β-diketone moiety absent deprotonation and boron coordination, we were curious to see if ligand films also showed spontaneous recovery at room temperature. The recovery time of dnmOMe was measured by smearing a thin film of the dye and monitoring the emission over time (Fig. 5). The peak emission of dnmOMe blue shifted immediately after smearing. After only ten minutes, the peak shifted from 503 nm (smeared state) to 445 nm. After one hour, the peak emission had entirely recovered to 440 nm, the peak emission in the annealed state. After a day, the FWHM of recovered dnmOMe thin films had decreased compared to the FWHM corresponding to the annealed sample (133 nm in TA vs 106 nm in recovered). This is opposite to the trend that is typically observed in BF_2bdks where the FWHM increases upon smearing and decreases upon annealing.[26] One possible explanation is that emission in the annealed state is broadened by emission from certain aggregate species formed during the fabrication of the film and mechanical stimulus is required to dissociate these species. This phenomenon has been observed in other mechanochromic materials where the mechanical grinding of certain tetraphenylethene powders was required in order to produce a wavelength change upon annealing.[37]

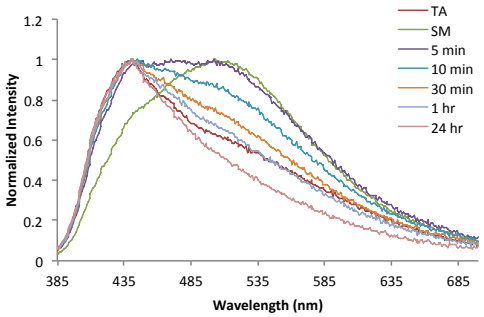

Fig 5. Emission spectral changes of dnmOMe thin film samples monitored over time after smearing (TA = thermally annealed; SM = smeared) (λ_{ex} = 369 nm).

Structural characterization was conducted by XRD, comparing annealed and smeared dnmOMe thin film patterns with those corresponding to the pristine powder (Fig 6). In the AS state, XRD patterns of dnmOMe thin films appeared amorphous. The crystallinity of dnmOMe in the annealed state was demonstrated by sharp peaks at ~13.4° and ~18.0°, which corresponded to peaks observed in the powder pattern of dnmOMe. When smeared, no peaks were observed, indicating that dnmOMe is amorphous in the smeared state.

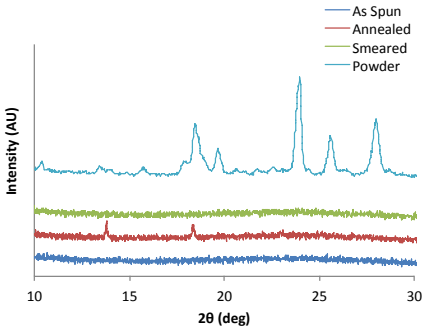

Fig 6. XRD spectra of dnmOMe as a powder, and thin films in the as spun, annealed, and smeared states.

AFM images of spin cast films in as spun, thermally annealed and recovered states were recorded in order to study the morphology of dnmOMe (Fig. 7). As spun films were used to approximate the morphology of the amorphous smeared state because quality images of smeared samples could not be obtained due to the fast rate of spontaneous recovery. The image of dnmOMe in the recovered state was obtained using a thin film one day after smearing to ensure the samples had entirely recovered prior obtaining images. In the as spun state, dnmOMe films were heterogeneous and showed plate-like features with large variation in size and shape. When annealed, dnmOMe formed both rod-like and plate-like crystallites. Compared to AS films, features are much larger with more defined shape post annealing. Images of dnmOMe after recovery showed much more disorder than both AS and TA films. Features were smaller overall, however a wider variance in particle size and shape is observed. These results are consistent with XRD patterns, which showed diffraction peaks for annealed samples but none were observed after smearing.

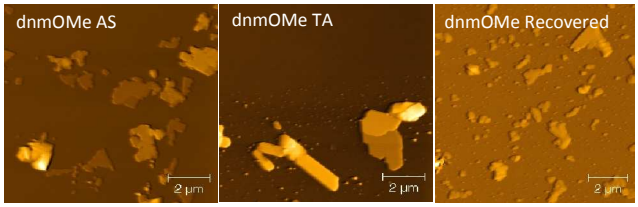

Fig 7. AFM images of dnmOMe films on glass substrates in as spun (AS), thermally annealed (TA) and recovered states.

Conclusions

In summary, the β-diketone dnmOMe showed unexceptional optical properties in methylene chloride solution, but a positive solvatochromic effect was observed when solvents were compared. AIE was demonstrated by measuring the emission of different THF/H_2O ratios. High contrast ML with rapid recovery was observed in dnmOMe thin films and structural characterization indicates that the emissive smeared state is amorphous while the non-emissive annealed state is crystalline. Because β-diketones are readily deprotonated to form diketonates, and can coordinate to metals and main group elements, this points to additional sensing possibilities for these responsive optical materials. Substituent effects on solid-state dinaphthoylmethane properties and comparison to corresponding boron complexes serve as subjects of future reports.

Acknowledgements

We thank the National Science Foundation (CHE GA11015) for support for this research. Dr. Jiwei Lu and Dr. Michal Sabat are acknowledged for their guidance with AFM and XRD measurements, respectively. We also thank Christopher DeRosa and Milena Kolpaczynska for their helpful assistance.

Notes and references

* Department of Chemistry, University of Virginia, Charlottesville, VA 22904, fraser@virginia.edu.

Electronic Supplementary Information (ESI) available: Synthesis, experimental details, and characterization data including thermal and optical measurements are provided in the ESI. See DOI: 10.1039/c000000x/

1 T. M. Figueira-Duarte and K. Müllen, *Chem. Rev.*, 2011, **111**, 7260.
2 S. Kim, J. Seo, H. K. Jung, J.-J. Kim and S. Y. Park, *Adv. Mater.*, 2005, **17**, 2077.
3 (a) Y. Qian, S. Li, G. Zhang, Q. Wang, S. Wang, H. Xu, C. Li, Y. Li and G. Yang, *J. Phys. Chem. B*, 2007, **111**, 5861 ; (b) K. R. Zbigniew, R. Grabowski, *Chem. Rev.*, 2003, **103**, 3899–4031.
4 (a) A. Pucci and G. Ruggeri, *J. Mater. Chem.*, 2011, **21**, 8282; (b) Z. C. X. Zhang, Y. Zhang, S. Liu, J. Xu, *J. Mater. Chem. C.*, 2013, **1**, 3376; (c) A. Pucci, R. Bizzarri and G. Ruggeri, *Soft Matter*, 2011, **7**, 3689; (d) K. Ariga, T. Mori and J. P. Hill, *Adv. Mater.,* 2012, **24**, 158.
5 (a) Y. Sagara, T. Komatsu, T. Ueno, K. Hanaoka, T. Kato and T. Nagano, *J. Am. Chem. Soc.*, 2014, **136**, 4273; (b) Y. Sagara and T. Kato, *Angew. Chem., Int. Ed.*, 2008, **47**, 5175; (c) Y. Sagara, S. Yamane, T. Mutai, K. Araki and T. Kato, *Adv. Funct. Mater.*, 2009, **19**, 1869.
6 (a) T. Wen, X.-P. Zhou, D.-X. Zhang and D. Li, *Chem. - Eur. J.*, 2014, **20**, 644; (b) Y. Chen, H. Zhang, X. Fang, Y. Lin, Y. Xu and W. Weng, *ACS Macr Lett.*, 2014, **3**, 141; (c) M. Kinami, B. R. Crenshaw and C. Weder, *Chem. Mater.*, 2006, **18**, 946; (d) C. Lowe and C. Weder, *Adv. Mater. (Weinheim, Ger.)*, 2002, **14**, 1625; (e) B. R. Crenshaw and C. Weder, *Chem. Mater.*, 2003, **15**, 4717.
7 (a) X.-C. Shan, F.-L. Jiamg, L. Chen, M.-Y. Wu, J. Pan, X.-Y. Wanab and M.-C. Hong, *J. Mater. Chem. C.*, 2013, **1**; (b) H. Ito, T. Saito, N. Oshima, N. Kitamura, S. Ishizaka, Y. Hinatsu, M. Wakeshima, M. Kato, K. Tsuge and M. Sawamura, *J. Am. Chem. Soc.*, 2008, **130**, 10044; (c) J. Ni, X. Zhang, N. Qiu, Y.-H. Wu, L.-Y. Zhang, J. Zhang and Z.-N. Chen, *Inorg, Chem.*, 2011, **50**, 9090; (d) R. Rao M, C.-W. Liao, *J. Mater. Chem. C.*, 2013, **1**, 6386.
8 W. Li, L. Wang, J.-P. Zhang and H. Wang, *J. Mater. Chem. C*, 2014, **2**, 1887.
9 (a) W. Z. Yuan, Y. Tan, Y. Gong, P. Lu, J. W. Y. Lam, X. Y. Shen, C. Feng, H. H. Y. Sung, Y. Lu, I. D. Williams, J. Z. Sun, Y. Zhang and B. Z. Tang, *Adv. Mater.*, 2013, **25**, 2837; (b) F. B. G. Prampolini, M. Biczysko, C. Cappelli, L. Carta, M. Lessi, A. Pucci, G. Ruggeri,V. Barone, *Chem. Eur. J.*, 2013, **19**, 1996 ; (c) Y. Ooyama, Y. Harima, *J. Mater. Chem.*, 2011, **21**, 8372; (d) Y. Gong, Y. Zhang, W. Z. Yuan, J. Z. Sun and Y. Zhang, *J. Phys. Chem. C*, 2014, **118**, 10998.
10 K. Nagura, H. Yusa, H. Yamawaki, H. Fujihisa, H. Sato, Y. Shimoikeda, and S. Yamaguchi, *J. Am. Chem. Soc.*, 2013, **135**, 10322.
11 R. Hu, N. L. C. Leung and B. Z. Tang, *Chem. Soc. Rev.*, 2014, **43**, 4494.
12 M. D. Watson, A. Fechtenkoetter and K. Muellen, *Chem. Rev. (Washington, D. C.)*, 2001, **101**, 1267.
13 J. Luo, Z. Xie, J. W. Y. Lam, L. Cheng, H. Chen, C. Qiu, H. S. Kwok, X. Zhan, Y. Liu, D. Zhu and B. Z. Tang, *Chem. Commun. (Cambridge, U. K.)*, 2001, 1740.
14 J. Chen, C. C. W. Law, J. W. Y. Lam, Y. Dong, S. M. F. Lo, I. D. Williams, D. Zhu and B. Z. Tang, *Chem. Mater.*, 2003, **15**, 1535.
15 (a) Y. Hong, J. W. Y. Lam and B. Z. Tang, *Chem. Commun. (Cambridge, U. K.)*, 2009, 4332; (b) T. He, X. T. Tao, J. X. Yang, D. Guo, H. B. Xia, J. Jia and M. H. Jiang, *Chem. Commun. (Cambridge, U. K.)*, 2011, **47**, 2907; (c) N. L. C. Leung, N. Xie, W. Yuan, Y. Liu, Q. Wu, Q. Peng, Q. Miao, J. W. Y. Lam and B. Z. Tang, *Chem. - Eur. J.*, 2014, **20**, 15349.
16 (a) Z. Ning, Z. Chen, Q. Zhang, Y. Yan, S. Qian, Y. Cao and H. Tian, *Adv. Funct. Mater.*, 2007, **17**, 3799; (b) H.-C. Su, O. Fadhel, C.-J. Yang, T.-Y. Cho, C. Fave, M. Hissler, C.-C. Wu and R. Reau, *J. Am. Chem. Soc.*, 2006, **128**, 983.
17 (a) Z. Chang, B. He, J. Chen, Z. Yang, P. Lu, H. S. Kwok, Z. Zhao, H. Qiua and B. Z. Tang, *Chem. Commun.*, 2013, **49**; (b) B. He, Z. Chang, Y. Jiang, X. Xu, P. Lu, H. S. Kwok, J. Zhou, H. Qiu, Z. Zhao and B. Z. Tang, *Dyes Pigm.*, 2014, **106**, 87.
18 J. Liu, Y. Zhong, J. W. Y. Lam, P. Lu, Y. Hong, Y. Yu, Y. Yue, M. Faisal, H. H. Y. Sung, I. D. Williams, K. S. Wong and B. Z. Tang, *Macromolecules*, 2010, **43**, 4921.
19 S. Shin, S. H. Gihm, C. R. Park, S. Kim, S. Y. Park, *Chem. Mater.*, 2013, **25**, 3288.
20 Y. Hong, J. W. Y. Lam and B. Z. Tang, *Chem. Soc. Rev.*, 2011, **40**, 5361.
21 (a) J. Liang, H. Shi, R. T. K. Kwok, M. Gao, Y. Yuan, W. Zhang, B. Z. Tang and B. Liu, *J. Mater. Chem. B*, 2014, **2**, 4363; (b) R. T. K. Kwok, J. Geng, J. W. Y. Lam, E. Zhao, G. Wang, R. Zhan, B. Liu and B. Z. Tang, *J. Mater. Chem. B*, 2014, **2**, 4134.
22 V. Bhalla, V. Vij, A. Dhir and M. Kumar, *Chem. – Eur. J.*, 2012, **18**, 3765.
23 C. Y. K. Chan, J. W. Y. Lam, Z. Zhao, S. Chen, P. Lu, H. H. Y. Sung, H. S. Kwok, Y. Ma, I. D. Williams and B. Z. Tang, *J. Mater. Chem. C*, 2014.
24 G. Zhang, J. P. Singer, S. E. Kooi, R. E. Evans, E. L. Thomas and C. L. Fraser, *J. Mater. Chem.*, 2011, **21**, 8295.
25 G. Zhang, J. Lu, M. Sabat and C. L. Fraser, *J. Am. Chem. Soc.*, 2010, **132**, 2160.
26 T.-D. Liu, A. D. Chien, J.-W. Lu, G.. Zhang and C. L. Fraser, *J. Mater. Chem.*, 2011, **21**, 8401.
27 N. D. Nguyen, G. Zhang, J.-W. Lu, A. E. Sherman and C. L. Fraser, *J. Mater. Chem.*, 2011, **21**, 8409.
28 W. A. Morris, T. Liu, and C. L. Fraser, *J. Mater. Chem. C.*, 2015 **3**, 352.
29 X. Sun, X. Li, S. Liu, G. Zhang, *J. Mater. Chem.* , 2012, **22**, 17332.
30 P. Galer, R. C. Korošec, M. Vidmar and B. Šket, *J. Am. Chem. Soc.*, 2014, **136**, 7383.
31 N. V. Belova, V. V. Sliznev, H. Oberhammer and G. V. Girichev, *J. Mol. Struct.*, 2010, **978**, 282.
32 (a) N. Mataga, Y. Kaifu and M. Koizumi, *Bull. Chem. Soc. Japan*, 1956, **29**, 465; (b) E. Lippert, *Z. Naturforsch.*, 1955, **10a**, 541.
33 X. Y. Shen, Y. J. Wang, E. Zhao, W. Z. Yuan, Y. Liu, P. Lu, A. Qin, Y. Ma, J. Z. Sun, B. Z. Tang, *J. Phys. Chem. C.*, 2013, **117**, 7334–7347.
34 G. Zhang, J. P. Singer, S. E. Kooi, R. E. Evans, E. L. Thomas, C. L. Fraser, *J. Mater. Chem. C.*, 2011, **21**, 8295.
35 J. Luo, L.-Y. Li, Y.-L. Song and J. Pei, *Chem. - Eur. J.*, 2011, **17**, 10515.
36 A. G. Mirochnik, B. V. Bukvetskii, E. V. Fedorenko, V. E. Karasev, *Russ.Chem.Bull., Int.Ed*, 2004, **53**, 279.
37 Y. Lv, Y. Liu, X. Ye, G. Liu and X. Tao, *CrystEngComm*, 2014.